ISSN: 1410-8917
e-ISSN: 2597-9914

Jurnal Kimia Sains dan Aplikasi 29 (2) (2026): 149-160

Jurnal Kimia Sains dan Aplikasi
Journal of Scientific and Applied Chemistry

Journal homepage: http://ejournal.undip.ac.id/index.php/ksa

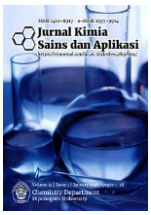

Synthesis of a Slow-Release Fertilizer Composite Based on Microcrystalline Cellulose from Coconut Husk Waste

Vicka Andini [1,*], Yoravika Dwiwibangga [1], Safniyeti [2], Nasywa Az Zahra [1], Ulfah Anis [3], Mega Elfia [1]

[1] Department of Chemistry, Faculty of Sciences and Mathematics, The University of Bengkulu, Bengkulu, Indonesia
[2] Department of Biology, Faculty of Sciences and Mathematics, The University of Bengkulu, Bengkulu, Indonesia
[3] Department of Agricultural Technology, Faculty of Agriculture, The University of Bengkulu, Bengkulu, Indonesia

* Corresponding author: vandini@unib.ac.id

https://doi.org/10.14710/jksa.29.2.149-160

Article Info

Article history:

Received: 15th December 2025
Revised: 14th February 2026
Accepted: 20th February 2026
Online: 14th March 2026

Keywords:
Microcrystalline cellulose; Coconut coir waste; Slow-release fertilizer; Biopolymer composite; Nutrient efficiency

Abstract

This study reports the synthesis and evaluation of a biodegradable slow-release fertilizer based on microcrystalline cellulose (MCC) extracted from coconut husk waste from Seluma Regency, Bengkulu Province. MCC was prepared through sequential acid washing, alkaline delignification, bleaching, and acid hydrolysis. A composite fertilizer was synthesized by incorporating maleate-containing polymer segments into MCC through limited radical grafting and/or esterification, followed by incorporation of polydihydroxymethylurea potassium phosphate (PDMU–KP) using citric acid as an interaction agent. Fourier transform infrared (FTIR) analysis indicates the presence of carbonyl, amide, and phosphate-related functional groups associated with the composite structure. Scanning electron microscopy (SEM) revealed a dense and agglomerated composite morphology with a rough, layered surface and crystalline aggregates, while energy-dispersive X-ray (EDX) analysis verified the presence of C, N, O, P, and K elements within the copolymer matrix. X-ray diffraction (XRD) analysis showed a reduction in cellulose crystallinity after copolymerization, indicating the formation of a polymer composite. Nutrient release tests conducted in distilled water for 28 days demonstrated controlled and differential release behavior governed by polymer swelling and matrix relaxation processes. Phosphate exhibited a maximum release concentration of 0.398 mg/L on day 7, followed by a gradual decrease to 0.058 mg/L by day 28. In contrast, nitrogen release occurred more gradually, reaching a maximum concentration of approximately 3.08 mg/L on day 14 before declining at later stages. These results indicate that the MCC-g-PMA/PDMU–KP copolymer provides sustained nutrient release with distinct release maxima for phosphorus and nitrogen, highlighting its potential as a cellulose-based slow-release fertilizer designed to improve nutrient use efficiency and reduce nutrient losses, derived from locally available coconut husk waste.

1. Introduction

Urea is widely used in Indonesia due to its high nitrogen content (~46%), which meets the substantial nitrogen demand of the agricultural sector. However, crops can only absorb a small fraction of this nitrogen, with a maximum uptake efficiency of around 35%, while the remainder is lost to the environment [1]. Most of the fertilizer applied in agricultural fields is carried away by water. Nitrogen can be transported via surface runoff or leach into the soil beyond the reach of plant roots (leachate) [2]. These losses not only increase production costs but also may have negative environmental impacts. Excessive fertilizer application can exacerbate the situation by causing nutrient imbalances, soil degradation, and environmental pollution. Therefore, to ensure long-term agricultural sustainability, the

implementation of efficient fertilization practices has become increasingly recognized as essential [3].

One innovative approach developed to address this challenge is the use of slow-release fertilizers (SRF). SRFs are fertilizer innovations that enable the gradual and controlled release of essential nutrients through chemical and microbiological mechanisms. This release system effectively mitigates uneven soil nutrient distribution, thereby optimizing nutrient availability for crops. Such fertilizers support plant growth by minimizing nutrient losses due to leaching or volatilization. Moreover, slow-release technology offers the advantage of releasing nutrients more efficiently and gradually compared to conventional fertilizers [3, 4]. However, many commercially available slow-release formulations are based on non-biodegradable polymers, which may raise environmental concerns and highlight the importance of developing biodegradable supporting materials [5]. Some formulations utilize coatings based on synthetic polymers, such as polyethylene–polyacrylic acid, polyacrylamide, and polyurethane. While these polymers are effective at delaying nutrient release, they raise sustainability concerns because microplastics remain in the soil after fertilizer application [6]. With the advancement of sustainable agricultural technologies, several studies have begun to explore natural materials as SRF matrices, including chitin, chitosan, and cellulose [7].

Microcrystalline cellulose (MCC) is a versatile biopolymer derived from plant cellulose [8]. MCC is produced through acid hydrolysis of plant cellulose fibers. It possesses high crystallinity and finer particle size than conventional cellulose, offering advantages in mechanical properties, biocompatibility, thermal stability, and biodegradability. These characteristics make MCC a highly promising material for the development of polymer composites and a suitable binding matrix for slow-release fertilizers [9, 10, 11]. MCC has attracted attention due to its high crystallinity, thermal stability, biocompatibility, and excellent biodegradability [12]. Studies on MCC derived from various biomasses, such as pomelo peel, bamboo, rice straw, oil palm fronds, banana peel, banana rachis, and lemongrass, have shown promising results for slow-release composite fertilizer applications [10, 11, 12, 13, 14, 15, 16, 17, 18]. Additionally, MCC can be sourced from abundant agricultural residues, such as coconut husk [19].

Seluma Regency is one of the coconut production centers in Bengkulu Province. According to the 2024 statistics from the Central Bureau of Statistics of Seluma Regency [20], Seluma contributes approximately 1,400 tons of coconut production in the western coastal region of Bengkulu, with an estimated coconut husk waste of over 150 tons per year. Unfortunately, this waste is not yet optimally utilized, with most being burned, charcoal, and adsorbents [21], or piled along the coast, leading to inefficient resource use and potential environmental burdens. When not properly managed, this lignocellulosic biomass tends to accumulate in open environments, leading to inefficient resource utilization and environmental concerns rather than providing added value. Uncontrolled disposal and natural decomposition of coconut husk waste may contribute to greenhouse gas emissions and local environmental degradation, while simultaneously representing a loss of potentially valuable renewable raw material [22].

From a sustainable waste management perspective, converting underutilized biomass residues into functional materials is an effective strategy to reduce environmental burdens while enhancing resource efficiency. Recent studies have emphasized that valorization of agricultural and coastal biomass waste into value-added products, such as polymeric or composite materials, can mitigate waste accumulation and reduce emissions associated with open dumping or uncontrolled degradation [19, 23]. According to Chand *et al.* [19], coconut husk contains approximately 35–45% cellulose, 40–45% lignin, and 5–10% hemicellulose. However, the chemical composition of coconut husk may vary depending on cultivar, geographical origin, maturity, and analytical method. Nevertheless, its relatively high lignocellulosic content makes it a suitable candidate for the production of MCC.

Urea-formaldehyde (UF)-based systems are among the most widely studied matrices for slow-release nitrogen fertilizers due to their hydroxymethylation–condensation chemistry, which enables gradual nitrogen release through controlled hydrolytic degradation. Recent developments have further explored UF–phosphate composite systems, in which phosphate incorporation can influence nitrogen release behavior and improve nutrient synchronization [2]. Building on this established UF fertilizer framework, the present study integrates a urea-formaldehyde-derived component (PDMU–KP) into a cellulose-based matrix to develop a biodegradable, slow-release fertilizer system. In this study, a slow-release fertilizer composite was developed by combining MCC extracted from coconut husk waste with MCC incorporating maleate-containing polymer segments and PDMU–KP. The approach emphasizes the utilization of locally available biomass resources and the incorporation of cellulose-based matrices to improve nutrient use efficiency and reduce nutrient losses. Citric acid was employed as a biobased interaction agent to facilitate interactions within the polymeric network.

2. Experimental

2.1. Tools and Materials

2.1.1. Materials for Synthesis

Coconut husks were obtained from local agricultural waste in Seluma Regency, Bengkulu Province, Indonesia. Hydrochloric acid (HCl, 37%, Merck), sodium hydroxide (NaOH, ≥98%, Merck), sodium chlorite ($NaClO_2$, 80%, HiMedia), and glacial acetic acid (CH_3COOH, ≥99.7%, Merck) were used for pretreatment, delignification, and bleaching processes during MCC preparation.

Maleic acid (≥99%, Merck), citric acid (≥99.5%, Merck), urea (≥99%, Merck), phosphoric acid (H_3PO_4, 85%, Merck), potassium dihydrogen phosphate (KH_2PO_4,

≥99%, Merck), formaldehyde solution (37%, Merck), potassium persulfate ($K_2S_2O_8$, ≥99%, Merck), ammonium persulfate ($(NH_4)_2S_2O_8$, ≥98%, Merck), and potassium hydroxide (KOH, ≥85%, Merck) were employed for copolymer synthesis. Absolute ethanol (≥99.8%, Merck) was used for washing and purification steps.

2.1.2. Materials for Nutrient Release Test

Commercial dialysis membranes (molecular weight cut-off 10–14 kDa) were used in the nutrient release experiments. Distilled water was used as the release medium and for all solution preparations. For phosphate determination based on SNI 06-6989.31-2005 (ascorbic acid method), ammonium molybdate tetrahydrate ($(NH_4)_6Mo_7O_{24}\cdot4H_2O$, ≥99%, Merck), potassium antimonyl tartrate ($K(SbO)C_4H_4O_6\cdot0.5H_2O$, ≥99%, Merck), ascorbic acid (≥99%, Merck), sulfuric acid (H_2SO_4, 95–98%, Merck), and potassium dihydrogen phosphate (KH_2PO_4, ≥99%, Merck) were used. For nitrogen (ammonia) determination following SNI 06-6989.30-2005 (phenate method), phenol (≥99%, Merck), sodium nitroprusside dihydrate ($Na_2[Fe(CN)_5NO]\cdot2H_2O$, ≥99%, Merck), sodium hypochlorite solution (NaOCl, 10–15% available chlorine, Merck), sodium hydroxide (NaOH, ≥98%, Merck), sodium citrate dihydrate ($C_6H_5Na_3O_7\cdot2H_2O$, ≥99%, Merck), and ammonium chloride (NH_4Cl, ≥99.5%, Merck) were employed. Distilled water was used for the preparation of reagents and standard solutions.

The main equipment utilized in this research comprised two-neck round-bottom flasks, volumetric flasks, beakers, measuring cylinders of various volumes, a magnetic stirrer with a heating plate, stir bars, glass funnels, spatulas, glass rods, a thermometer, a pH meter, an analytical balance, a grinder (blender), an oven, a desiccator, and an 18-mesh sieve. For characterization, the instruments used included an FTIR (Bruker Alpha I) for functional group identification, an XRD (Bruker D6 Phaser) for crystallinity analysis, and an SEM (Thermo Scientific Phenom ProX G6 Desktop) for surface morphology observation. Additional apparatus used in the nutrient release study included plastic pots, dialysis bags, 250 mL Erlenmeyer flasks, and a UV-Vis Spectrophotometer for nutrient quantification. All glassware was thoroughly cleaned and oven-dried prior to use to ensure experimental accuracy.

2.2. Preparation of Coconut Husk Powder

The mesocarp (coconut husk) was separated from the exocarp using a knife. The coconut coir was then cleaned to remove coarse impurities such as soil and remaining exocarp residues. The cleaning process was carried out using running water to eliminate dust, soil, and other organic contaminants. After cleaning, the husks were sun-dried for two days to reduce their moisture content. During this process, the material became lighter in color and more fibrous. This was followed by oven drying at 60-70°C to ensure complete dryness. The dried husks were then cut into small pieces and ground using a blender until a fine powder was obtained. The powder was sieved through an 18-mesh sieve to achieve a uniform particle size. The prepared coconut husk powder was subsequently used for the extraction of microcrystalline cellulose (MCC) [17, 19].

2.3. Extraction of Microcrystalline Cellulose (MCC)

MCC was extracted from local coconut coir waste according to the methods reported by Zhang *et al.* [10] and Krishnan *et al.* [24], with slight modifications. Initially, 20.0 g of the sieved coconut coir powder was subjected to acid washing using 600 mL of 0.1 mol/L HCl solution under continuous stirring to remove mineral impurities and soluble components. The mixture was filtered, washed with distilled water until neutral pH, and dried at 60°C. The dried material was then treated with 400 mL of 10% (w/w) NaOH solution, heated, and stirred for 3 h to remove lignin and hemicellulose. The solid was filtered, washed with distilled water until neutral, and dried again. Subsequently, the alkali-treated cellulose was bleached using a mixture of 200 mL of 1% (w/v) $NaClO_2$ solution and 2 mL of glacial acetic acid at 80°C for 2 h under continuous stirring. The bleached cellulose was filtered, washed three times with distilled water and absolute ethanol, and dried at 60°C.

MCC was then prepared from the bleached cellulose through acid hydrolysis. The dried bleached cellulose was treated with 2.5 M HCl at 85°C for 60 min using a solid-to-liquid ratio of 1:10 (w/v). After hydrolysis, the mixture was cooled to room temperature, filtered, and washed with distilled water until pH 7. The obtained MCC was oven-dried at 80°C until a constant weight was achieved. The final MCC powder was stored in a desiccator prior to use as the main biopolymer matrix in the synthesis of the slow-release fertilizer composite.

2.4. Synthesis of Polydihydroxymethylurea Potassium Phosphate (PDMU-KP)

Urea (6.0 g) was dissolved in 15 mL of distilled water in a two-neck round-bottom flask, followed by the addition of 1.4 mL of 37% formaldehyde solution. The mixture was stirred at room temperature for approximately 15 min until a homogeneous solution was obtained. The pH of the mixture was adjusted to 9.0 by the dropwise addition of 1 M KOH solution under continuous stirring, and the reaction was maintained at 40°C for 2 h to form dihydroxymethylurea (DMU). The pH of the reaction mixture was then lowered to approximately 3.0 using 1 M HCl solution added dropwise. After pH adjustment, 6.8 g (0.05 mol) of KH_2PO_4 was added to the acidic mixture, followed by stirring for 60 min to ensure complete homogenization. The resulting solution was transferred to a sealed reaction vessel and incubated at 120°C for 3 h to complete the polycondensation process. In this step, KH_2PO_4 acted as a nutrient source and structural modifier and was incorporated into the urea–formaldehyde matrix primarily through ionic interactions and physical entrapment during polycondensation, rather than through covalent phosphate ester formation. The obtained solid product, identified as polydihydroxymethylurea potassium phosphate (PDMU-KP), was dried in an oven at 70°C, ground, and sieved to yield fine white particles. This procedure was conducted with slight modifications from the method reported by Wang *et al.* [14].

2.5. Synthesis of Microcrystalline Cellulose-g-Poly(Maleic Acid)/Polyhydroxymethylurea Potassium Phosphate (MCC-g-PMA/PDMU–KP) Copolymer Using Citric Acid

The synthesis of microcrystalline cellulose-g-poly(maleic acid)/polyhydroxymethylurea potassium phosphate (MCC-g-PMA/PDMU–KP) copolymer using citric acid was adapted from the method described by Wang *et al.* [14], with major modifications in monomer composition, interaction agent, and reaction conditions. MCC (2.0 g) was placed in a two-neck round-bottom flask and mixed with maleic acid solution (4.0 g), which had been partially neutralized with 1 M KOH to adjust the pH to 6.0–6.5. The mixture was stirred using a magnetic stirrer until homogeneous. Subsequently, urea (2.0 g) was added, and stirring was continued for 15 min at room temperature to ensure uniform mixing.

Potassium persulfate (KPS) and ammonium persulfate (APS) (0.2 g each) were dissolved in 10 mL of distilled water and then added to the reaction mixture as initiators. The system was gradually heated to 80°C under gentle stirring (200 rpm). At this stage, citric acid (0.5 g) was added as an interaction agent. After complete dissolution, 0.1 M phosphoric acid solution was added dropwise while monitoring the pH until it reached 2–3, providing conditions favorable for esterification and possible limited grafting reactions.

Next, PDMU–KP (1.5 g) was added to the reaction mixture, and the system was maintained at 80°C for 3 h to allow polymerization and possible limited grafting and esterification interactions. Upon completion, the mixture was allowed to cool to room temperature and filtered if necessary. The solid product was oven-dried at 70°C for approximately 6 h until a constant weight was obtained. The resulting pale-yellow powder was identified as microcrystalline cellulose-g-poly(maleic acid)/PDMU–KP copolymer (MCC-g-PMA/PDMU–KP).

2.6. Characterization of the Synthesized Products

The synthesized composite fertilizer was characterized using Fourier transform infrared spectroscopy (FTIR) to identify the main chemical functional groups and confirm copolymer formation, scanning electron microscopy coupled with energy-dispersive X-ray spectroscopy (SEM-EDX) to observe surface morphology and elemental composition, and X-ray diffraction (XRD) to analyze the crystal structure of microcrystalline cellulose and the changes occurring after chemical modification. The crystallinity index (CrI) was estimated from XRD patterns using the Segal method, based on the relative intensities of the crystalline (002) peak and the amorphous background. These characterization techniques were employed to verify the success of the synthesis process and to elucidate the structure of the resulting material as a slow-release fertilizer.

2.7. Nutrient Release Test in Aqueous Medium

A total of 0.2 g of the sample was placed into a commercial dialysis membrane with a molecular weight cut-off (MWCO) of 10–14 kDa and immersed in 200 mL of distilled water contained in an Erlenmeyer flask. The semi-permeable membrane allows the free diffusion of low-molecular-weight nutrient ions (e.g., NH_4^+ and PO_4^{3-}) while retaining the solid polymer matrix inside the dialysis membrane. At specific time intervals (1, 7, 14, 21, and 28 days), 10 mL of the solution was withdrawn for analysis of nutrient content, including nitrogen (N) and phosphorus (P). To maintain a constant volume, 10 mL of fresh distilled water was added after each sampling. The elemental concentrations in the samples were determined using a UV–Vis spectrophotometer [14].

Phosphate (P) concentrations were determined using the ascorbic acid method following SNI 06-6989.31-2005, with absorbance measured at 880 nm and a working calibration range of 0.01-1.0 mg P L^{-1}, which fully covers the measured sample concentrations (≤0.40 mg L^{-1}). Ammonium (NH_4^+) concentrations were analyzed using the phenate spectrophotometric method following SNI 06-6989.30-2005, with absorbance measured at 640 nm and a working range of 0.1-0.6 mg NH_3-N L^{-1}, which covers the measured concentrations. When measured concentrations exceeded the linear range of the calibration curve, appropriate dilution was performed before analysis to ensure accurate quantification.

3. Results and Discussion

3.1. Preparation for Coconut Husk Powder

Pretreatment of the coconut husk successfully produced fine, uniform powder suitable for subsequent cellulose extraction. This result was achieved through a series of steps, as shown in Figure S1, which shows the appearance of the coconut fiber after the sun-drying process. Subsequent oven drying resulted in a brittle texture that facilitated mechanical grinding. The subsequent oven drying produced a brittle texture that facilitated mechanical grinding. After milling, the material turned into a fine brownish powder (Figure S2), showing that the fibers had been effectively broken down into smaller fragments. The sieving step using an 18-mesh screen produced uniformly sized particles (Figure S3), improving the homogeneity of the material and increasing its surface area for chemical reactions during cellulose extraction. The gradual color change from dark brown (raw husk) to light brown (dried and sieved powder) indicates the removal of surface impurities such as dust during washing and drying. Overall, this pretreatment process yielded clean, stable, and homogeneous coconut husk powder, providing a consistent, reactive substrate for MCC extraction.

3.2. Extraction of Microcrystalline Cellulose (MCC)

The extraction process removed non-cellulosic components from coconut coir powder through acid washing, alkaline delignification, bleaching, and acid hydrolysis. Acid washing with 0.1 M HCl dissolved mineral salts, waxes, and other water-soluble impurities, as reported by Poornachandhra *et al.* [25], leading to a slight color change from brown to light yellowish-brown. Subsequent treatment with 10% NaOH resulted in a noticeable darkening of the material to a deep brown

color, indicating partial lignin solubilization and possible condensation reactions of residual lignin under alkaline conditions. According to Abolore *et al.* [26], alkaline pretreatment using NaOH effectively disrupts lignin–carbohydrate linkages and removes hemicellulose by saponifying ester bonds, thereby enhancing cellulose accessibility for subsequent reactions. Despite the darker appearance, this step successfully disrupted lignin–carbohydrate complexes and removed most of the hemicellulose fraction. The bleaching stage using $NaClO_2$ and glacial acetic acid produced a light beige cellulose sample, suggesting extensive removal of lignin residues. The reaction between chlorite and acetic acid generated chlorine dioxide, a strong oxidizing agent that selectively delignified the cellulose fibers without significant degradation of the polysaccharide backbone.

Finally, acid hydrolysis with 2.5 M HCl yielded fine, crystalline MCC particles with improved purity and reduced amorphous regions. The high temperature (85°C) and short reaction time (30 min) favored controlled depolymerization of amorphous cellulose, resulting in microcrystalline fragments. The final MCC powder was white, odorless, and smooth in texture, indicating successful removal of non-cellulosic impurities. The obtained MCC served as a biopolymer matrix for the subsequent synthesis of the slow-release fertilizer composite. The appearance of the obtained MCC is shown in Figure S4, which displays the fine, pale white powder characteristic of purified microcrystalline cellulose derived from coconut coir. The yield of MCC was determined by gravimetric analysis using Equation (1).

$$\text{MCC yield } (wt\%) = \frac{m\text{MCC}}{m\text{Raw Coir}} \times 100 \quad (1)$$

Where, *m*MCC is the dry mass of microcrystalline cellulose obtained after acid hydrolysis, and *m*Raw Coir is the initial dry mass of coconut coir used in the purification process. In this study, 20.0 g of dried coconut coir was subjected to sequential alkaline treatment, bleaching, and acid hydrolysis, resulting in 7.2 g of dried MCC. Therefore, the MCC yield was calculated using Equation (2).

$$\text{MCC yield } (wt\%) = \frac{7.2}{20.0} \times 100 = 36\% \quad (2)$$

This yield is consistent with the reported cellulose content of coconut coir (35–45 wt%) and indicates effective removal of lignin, hemicellulose, and amorphous cellulose fractions during the purification process, while preserving the crystalline cellulose domains.

3.3. Synthesis of Polydihydroxymethylurea Potassium Phosphate (PDMU–KP)

The polycondensation of urea, formaldehyde, and potassium dihydrogen phosphate resulted in the formation of a fine white polymeric product, identified as PDMU–KP. The reaction mechanism involves two key stages: (i) formation of dihydroxymethylurea (DMU) through the hydroxymethylation of urea by formaldehyde under alkaline conditions, and (ii) subsequent condensation under acidic and thermal conditions to form a crosslinked urea–formaldehyde polymer matrix with incorporated phosphate species, predominantly through ionic association and physical entrapment.

During synthesis, pH adjustment played a crucial role in directing the reaction pathway. Under basic conditions (pH 9), the urea–formaldehyde reaction promoted the formation of hydroxymethyl intermediates, while lowering the pH to 3 favored condensation and phosphate incorporation. The final heating at 120°C for 3 h ensured complete polymerization, yielding a stable, insoluble, and uniform PDMU–KP powder. According to Wang *et al.* [14] and Xiang *et al.* [27], the incorporation of phosphate groups into polymer matrices enhances structural stability, water retention, and the controlled release of nutrients in slow-release fertilizer systems. The presence of phosphate groups in PDMU–KP introduces ionic sites capable of forming hydrogen bonds and electrostatic interactions with the cellulose matrix during subsequent composite formation. These features make PDMU–KP a promising nitrogen–phosphorus source for sustainable slow-release fertilizers, combining nutrient functionality with biodegradable polymeric behavior. The appearance of the synthesized PDMU–KP is shown in Figure S5, displaying a fine, white polymeric powder with uniform texture and no visible agglomeration.

3.4. Synthesis of Microcrystalline Cellulose-g-Poly(Maleic Acid)/Polyhydroxymethylurea Potassium Phosphate (MCC-g-PMA/PDMU–KP) Copolymer Using Citric Acid

The introduction of citric acid played a dual role as an interaction agent, promoting strong hydrogen bonding and possible limited ester formation with hydroxyl groups in the cellulose and polymer matrices, thereby enhancing structural integrity. In addition, citric acid may facilitate esterification reactions by providing an acidic environment, which is consistent with reported interaction-assisted network formation in citric acid-modified biopolymeric systems [28, 29]. The presence of initiators (KPS and APS) efficiently generated free radicals that promoted the formation of polymer segments associated with MCC, possibly involving limited grafting, esterification, and strong intermolecular interactions, producing a stable composite structure. After drying, the obtained MCC-g-PMA/PDMU-KPP exhibited a pale-yellow to light-beige color, a finer particle morphology, and a slightly cohesive texture, indicating successful copolymerization and chemical bonding among the components.

Maleic acid has been reported to enable covalent bonding between polymer backbones and cellulose primarily through radical-mediated grafting under appropriate conditions, although esterification and strong intermolecular interactions may also contribute significantly [30]. In the present system, the resulting copolymer exhibited improved compatibility between the cellulose and phosphate–urea polymer phase, which is expected to enhance nutrient retention and provide slow-release behavior in subsequent fertilizer formulations. The physical appearance of the final product is shown in Figure S6; the copolymer appeared as a uniform pale-yellow powder, distinct from the white MCC precursor,

suggesting interactions between the polymer and cellulose segments, possibly including limited grafting and esterification, rather than conclusively proving extensive covalent bonding.

3.5. FTIR Characterization

FTIR characterization was performed over the wavenumber range of 4000–500 cm^{-1} for four samples: coconut husk, MCC, PDMU-KP, and the MCC-g-PMA/PDMU–KP composite. The spectra are compared in Figure 1. The FTIR spectrum of coconut husk shows a broad band at 3400–3200 cm^{-1} attributed to O–H stretching from cellulose, hemicellulose, and lignin. The band at ~2922 cm^{-1} arises from aliphatic C–H stretching (–CH and $–CH_2$) of the polysaccharide backbone (Figure 1a). A sharp band around 1732 cm^{-1} is associated with C=O stretching vibrations of acetyl and uronic ester groups in hemicellulose as well as ester groups in lignin. Meanwhile, bands at approximately 1609 and 1518 cm^{-1} correspond to aromatic C=C skeletal vibrations characteristic of lignin. The band near 1247 cm^{-1} indicates C–O stretching vibrations of aryl–ether linkages in lignin, whereas the strong bands at 1050–1030 cm^{-1} are assigned to C–O–C and C–O stretching vibrations of cellulose and hemicellulose. The presence of these characteristic bands confirms that coconut husk is a lignocellulosic biomass with a relatively high content of lignin and hemicellulose [31].

After acid washing, alkaline delignification, bleaching, and acid hydrolysis, the FTIR spectrum of MCC shows significant changes compared to that of raw coconut husk (Figure 1b). The broad O–H stretching band at 3400–3200 cm^{-1} and the C–H stretching band around 2889 cm^{-1} remain present, indicating that the cellulose backbone is preserved. However, the C=O band at approximately 1724 cm^{-1} and the lignin-related aromatic bands at 1625 and 1592 cm^{-1} are markedly reduced, suggesting that most hemicellulose and lignin were successfully removed during the pretreatment process. In the fingerprint region (1500–800 cm^{-1}), cellulose bands become more pronounced, including ~1430 cm^{-1} (CH_2 bending, crystallinity band), 1370 cm^{-1} (C–H bending), 1321 cm^{-1} (CH_2 wagging), and strong bands at ~1157, 1026, and 895 cm^{-1}. These correspond to C–O–C stretching (glycosidic linkages), C–O stretching of secondary alcohols, and β-glycosidic C–H out-of-plane vibrations, respectively. The sharper and better-resolved bands indicate increased molecular order and cellulose crystallinity, consistent with MCC characteristics [32].

The FTIR spectrum of PDMU–KP is presented in Figure 1c. A broad absorption band at 3440 and 3325 cm^{-1} is observed, which is attributed to overlapping O–H and N–H stretching vibrations from hydroxymethyl and amide groups. The band at 2955 cm^{-1} corresponds to aliphatic C–H stretching of methylene groups formed during the urea–formaldehyde reaction. A strong absorption band at 1642 cm^{-1} is assigned to C=O stretching vibrations (amide I) of the polydihydroxymethylurea backbone, while the band at 1551 cm^{-1} is attributed to N–H bending coupled with C–N stretching (amide II). The band observed at 1346 cm^{-1} is associated with C–N stretching vibrations of the urea-based polymer network. Intense bands appearing at 1133 and 1026 cm^{-1} are attributed to P–O and C–O–P stretching vibrations of phosphate groups, confirming the incorporation of KH_2PO_4 into the polymer matrix. Additionally, the band observed at 1264 cm^{-1} is assigned to the P=O stretching vibration, consistent with reported phosphate spectra. Additionally, the band at 895 cm^{-1} is attributed to –P–O bending vibrations of dihydrogen phosphate species. The simultaneous presence of amide and phosphate bands confirms the successful formation of a PDMU–KP rather than a simple physical mixture [14].

As shown in Figure 1d, the FTIR spectrum of the MCC-g-PMA/PDMU–KP copolymer exhibits a broad O– H/N–H stretching band in the region of 3400–3200 cm^{-1}, whose intensity is reduced and slightly shifted toward lower wavenumbers compared to pristine MCC. This change suggests the involvement of cellulose hydroxyl (– OH) groups in enhanced intermolecular interactions within the composite matrix, possibly through esterification reactions with maleic acid and citric acid rather than remaining entirely as free hydroxyl groups.

In the carbonyl region, a discernible absorption band is observed at approximately 1720–1710 cm^{-1}, which is assigned to C=O stretching vibrations of ester (–COO–) groups, consistent with ester linkages that may result from limited grafting and/or esterification reactions. Importantly, free maleic acid typically exhibits dominant carboxylate-related bands at ~1637 and ~1389 cm^{-1}, along with a very broad carboxylic O–H stretching band in the 3300–2500 cm^{-1} region [33]. Similarly, free citric acid shows strong and broad O–H absorption and carbonyl features associated with carboxylic acid groups [34, 35]. These characteristic features are absent in the MCC-g-PMA/PDMU–KP spectrum. Before FTIR characterization, the samples were repeatedly washed with water and ethanol, indicating that residual free carboxylic acids were minimal. Therefore, the contribution of the band at ~1720–1710 cm^{-1} is more reasonably associated with ester-related C=O stretching within the composite structure rather than unreacted carboxylic acid groups.

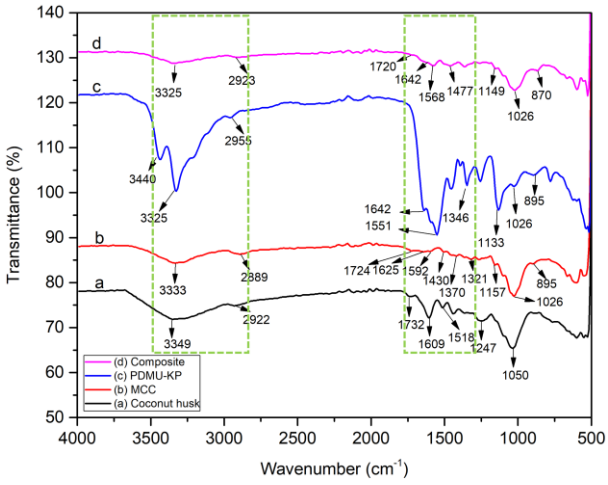

Figure 1. FTIR spectra of (a) Coconut husk, (b) MCC, (c) PDMU–KP, and (d) MCC-g-PMA/PDMU–KP composite

The amide I and amide II bands originating from the PDMU–KP segments remain observable at around 1642 and 1568 cm^{-1}, respectively, indicating that the polydihydroxymethylurea backbone is retained within the composite structure. In the fingerprint region, phosphate-related P–O and P=O bands in the range of 1149–870 cm^{-1} overlap with the C–O–C vibrations of cellulose, resulting in broader and more complex absorption features. Meanwhile, the cellulose crystallinity band at approximately 1477 cm^{-1} shows a slight decrease in intensity compared to pristine MCC, suggesting partial disruption of the crystalline domains due to the incorporation of polymer segments and associated intermolecular interactions, possibly involving limited grafting and esterification, without completely destroying the cellulose structure.

3.6. SEM–EDX Characterization

The surface morphologies of coconut husk, MCC, PDMU–KP, and the MCC-g-PMA/PDMU–KP copolymer were examined using a scanning electron microscope (Thermo Fisher Scientific Phenom ProX G6 Desktop SEM). This analysis aimed to observe changes in the physical structure of the materials at each synthesis stage and to evaluate the relationship between composite morphology and nutrient release mechanisms. Observations were conducted at 3000× magnification with an accelerating voltage of 5 kV, using a backscattered electron detector (BSD). The resulting micrographs are presented in Figure 2.

SEM images of coconut husk reveal a surface structure composed of large, sheet-like layers that are curled and form a rough, non-homogeneous texture with numerous folds and wrinkles (Figure 2a). The surface is covered by an amorphous layer originating from a mixture of lignin, hemicellulose, and other impurities that remain attached to the fibers. The presence of these thick, layered structures indicates that the lignocellulosic cell walls have not yet undergone chemical degradation. This observation is consistent with the characteristics of raw biomass, which is rich in lignin and hemicellulose [36]. EDX analysis of the coconut husk surface indicates that the material is primarily composed of carbon and oxygen, consistent with its lignocellulosic nature, as shown in Table 1.

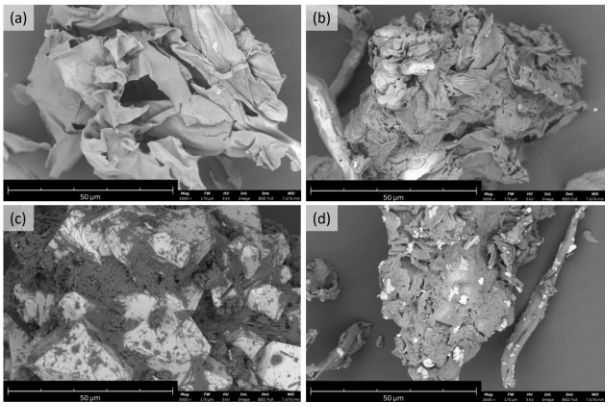

Figure 2. Surface morphologies of the samples: (a) coconut husk, (b) MCC, (c) PDMU–KP, and (d) MCC-g-PMA/PDMU–KP copolymer

In the analyzed region, carbon (45.60 wt%) and oxygen (47.10 wt%) were the dominant detected elements. Minor elements such as magnesium (0.10 wt%), phosphorus (0.60 wt%), and chlorine (6.60 wt%) were also observed, likely from natural mineral impurities or surface residues. EDX provides surface-sensitive, semi-quantitative elemental data, and values may vary across analyzed spots due to the heterogeneity of lignocellulosic materials. Therefore, the results mainly confirm elemental presence rather than precise bulk composition. The spectra are shown in Figure S7.

After delignification, bleaching, and acid hydrolysis, the morphology of MCC shows significant changes compared to that of coconut husk. The surface structure appears cleaner and more homogeneous, displaying cellulose fragments that have peeled into thinner sheet-like structures. The MCC surface also appears more brittle, with fine cracks, indicating degradation of the lignocellulosic structure and an increase in cellulose content. No thick amorphous layers similar to those observed in coconut husk are detected, confirming that most lignin and hemicellulose have been effectively removed, as shown in Figure 2b. This morphology is consistent with the FTIR results, which show the disappearance of hemicellulose C=O peaks and lignin-related aromatic peaks [37].

EDX analysis of MCC shows that the sample is dominated by carbon (71.50%), followed by oxygen (28.50%). This composition is consistent with the characteristics of pure cellulose, in which the β-1,4-glucan polymer backbone is composed of glucopyranose units rich in hydroxyl (–OH) groups and C–O–C linkages. No inorganic elements such as Mg, Cl, or P are detected, indicating that the delignification and purification processes successfully removed most mineral contaminants and residual lignin typically present in the original biomass. These results confirm that the obtained MCC has high purity and is suitable for use as a substrate for subsequent processes, including copolymer formation involving possible limited grafting and esterification. The elemental composition of MCC based on EDX analysis is presented in Table 2, while the corresponding EDX spectrum is shown in Figure S8.

Table 1. Elemental composition obtained from EDX analysis of coconut husk samples

Element	Symbol	Weight (%)	Atomic (%)
Carbon	C	45.60	54.629
Oxygen	O	47.10	42.355
Magnesium	Mg	0.100	0.059
Phosphorus	P	0.600	0.279
Chlorine	Cl	6.600	2.678

Table 2. Elemental composition obtained from EDX analysis of MCC samples

Element	Symbol	Weight (%)	Atomic (%)
Carbon	C	71.500	76.97
Oxygen	O	28.500	23.03

Table 3. Elemental composition obtained from EDX analysis of PDMU–KP samples

Element	Symbol	Weight (%)	Atomic (%)
Carbon	C	2.200	4.220
Nitrogen	N	14.400	23.680
Oxygen	O	25.100	36.142
Phosphorus	P	10.400	7.734
Potassium	K	47.900	28.224

Table 4. Elemental composition obtained from EDX analysis of MCC-g-PMA/PDMU–KP samples

Element	Symbol	Weight (%)	Atomic (%)
Carbon	C	6.294	13.780
Nitrogen	N	1.299	2.438
Oxygen	O	22.178	36.450
Phosphorus	P	0.400	0.339
Sulphur	S	0.200	0.164
Potassium	K	69.630	46.829

The PDMU–KP sample in Figure 2c exhibits a morphology that is markedly different from that of MCC and coconut husk. In the SEM images, PDMU–KP appears as large blocky, crystalline-like structures with bright surfaces when observed using a BSD detector. On the surfaces of these regions, thin polymer layers as well as filaments and small particles are irregularly attached. These morphological features suggest a hybrid system in which phosphate-rich regions are associated with an organic polymer matrix formed through urea polycondensation. The presence of large blocky domains is consistent with the formation of phosphate-modified urea polycondensation products, as also supported by the FTIR spectra [38].

EDX analysis of PDMU–KP reveals the presence of C, N, O, P, and K elements, which represent the constituent components of the material. Nitrogen, oxygen, and phosphorus are associated with the amide groups, hydroxymethyl groups, and phosphate groups within the phosphate–urea polymer structure. Carbon originates from the organic urea component, while potassium serves as a counter cation for the phosphate groups within the polymer network. This elemental composition reflects the chemical structure of PDMU–KP formed through the reaction of urea, formaldehyde, and potassium dihydrogen phosphate. The elemental composition of PDMU–KP based on EDX analysis is summarized in Table 3, while the corresponding EDX spectrum is presented in Figure S9.

Furthermore, the morphology of the MCC-g-PMA/PDMU–KP copolymer in Figure 2d exhibits a surface structure that is considerably more complex than that of pristine MCC and PDMU–KP. SEM images show that MCC fragments are no longer visible as clean sheet-like structures, as observed in pristine MCC, indicating that the cellulose surface is covered by a non-uniform polymeric layer formed through polymer deposition and interactions with the PDMU–KP phase, possibly involving limited grafting and esterification. The composite exhibits a compact, agglomerated morphology with a rough, layered surface structure. Such a dense morphology is expected to restrict rapid water penetration into the composite matrix, which is consistent with the delayed nitrogen release behavior observed in the aqueous release study.

In addition, the composite surface exhibits bright, dispersed regions distributed throughout the matrix. In the absence of elemental mapping analysis, these features are more appropriately described as dispersed crystalline aggregates rather than being explicitly assigned to phosphate-containing domains. The presence of these aggregates, together with the polymer-coated cellulose framework, contributes to a heterogeneous, compact composite structure that may influence water diffusion and the gradual release of nutrients.

EDX analysis of the MCC-g-PMA/PDMU–KP copolymer confirms the presence of C, N, O, P, S, and K elements, representing all constituent components of the composite. Carbon and oxygen originate from MCC, maleic acid, and PDMU-KP, while nitrogen is derived from PDMU–KP since MCC and PMA contain no nitrogen. Phosphorus and potassium indicate the phosphate component of PDMU–KP formed from KH_2PO_4 during synthesis. The simultaneous detection of these elements within the same analyzed area indicates the coexistence and successful integration of MCC, PMA, and PDMU–KP on the composite surface, consistent with the formation of a true composite material. The elemental composition of MCC-g-PMA/PDMU–KP based on EDX analysis is presented in Table 4, while the corresponding EDX spectrum is shown in Figure S10.

Based on the EDX atomic percentages, the N:P ratio of the MCC-g-PMA/PDMU–KP composite was approximately 7.2:1. It should be emphasized that EDX provides semi-quantitative elemental information from a localized surface region rather than the bulk composition of the material. Therefore, the relatively high potassium content observed in the analyzed area does not necessarily represent the overall stoichiometry of the composite. The marked difference between K and P weight percentages may indicate local phase heterogeneity or partial segregation of potassium-rich crystalline domains within the polymer matrix. Consequently, the EDX results reflect surface-local elemental distribution rather than the true bulk composition of the MCC-g-PMA/PDMU–KP composite.

3.7. XRD Characterization

XRD patterns of the four samples exhibit distinct changes in crystalline structure corresponding to each treatment stage (Figure 3). Raw coconut husk exhibits a broad diffraction pattern with relatively low intensity, indicating a dominant amorphous fraction, likely due to lignin and hemicellulose in the natural biomass. After extraction and acid hydrolysis, MCC shows a pronounced increase in diffraction intensity at around 22° (2θ), which is characteristic of crystalline cellulose domains, indicating enhanced cellulose purity and crystallinity compared to the original coconut husk.

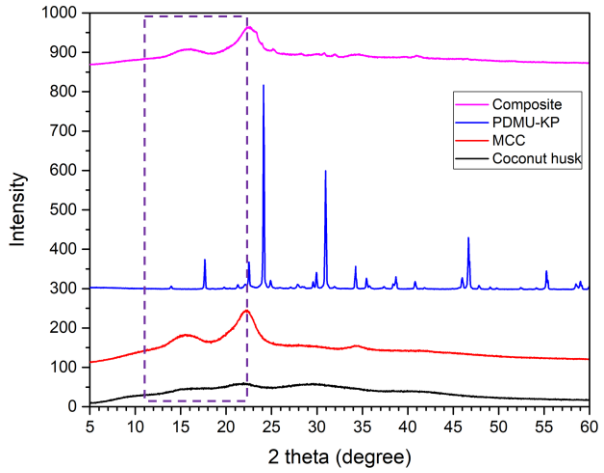

Figure 3. XRD patterns of coconut husk, MCC, PDMU–KP, and MCC-g-PMA/PDMU–KP composite

The PDMU–KP polymer exhibits several sharp diffraction reflections, indicating its semicrystalline nature arising from the phosphate-modified urea–formaldehyde structure. This diffraction pattern differs markedly from that of cellulose, confirming the presence of an ordered polymer phase. Upon copolymer formation (MCC-g-PMA/PDMU-KP), the XRD pattern changes significantly: the sharp crystalline peaks associated with PDMU-KP are weakened or become less discernible, and the diffraction region around 22-23° becomes broader with an overall reduction in intensity. These changes indicate disruption of crystalline order and reduced overall crystallinity, suggesting increased amorphization. This behavior is consistent with intermolecular interactions and incorporation of polymer segments within the MCC matrix, possibly involving limited grafting and esterification, which partially disturb crystalline domains rather than forming a fully ordered structure. Consequently, the amorphous fraction of the composite increases.

3.8. Nutrient Release Test in Aqueous Medium

The release of phosphate and nitrogen from the MCC-g-PMA/PDMU-KP copolymer was analyzed using a UV-Vis spectrophotometer, following standardized procedures based on SNI 06-6989.31-2005 for phosphate determination (ascorbic acid method) and SNI 06-6989.30-2005 for nitrogen determination (phenate method). The use of these national standards ensures that nutrient quantification is performed using verified calibration systems, wavelengths, and reagent protocols, thereby providing reliable and accurate data.

Table 5. Average phosphate concentrations (mg/L) in distilled water during a 28-day release test of MCC-g-PMA/PDMU–KP

Day	Duplicate 1 (mg/L)	Duplicate 2 (mg/L)	Average (mg/L)
1	0.287	0.226	0.257
7	0.388	0.407	0.398
14	0.127	0.128	0.128
21	0.066	0.070	0.068
28	0.053	0.063	0.058

Table 6. Average nitrogen concentrations (mg/L) in distilled water during a 28-day release test of MCC-g-PMA/PDMU–KP

Day	Duplicate 1 (mg/L)	Duplicate 2 (mg/L)	Average (mg/L)
1	1.321	1.397	1.359
7	2.119	2.073	2.096
14	3.090	3.070	3.080
21	2.465	2.465	2.465
28	1.230	1.365	1.298

Phosphate release exhibited a relatively rapid diffusion pattern during the initial observation period. The highest phosphate concentration was observed on day 7, with duplicate values of 0.388 and 0.407 mg/L, yielding an average concentration of 0.398 mg/L. The increase up to day 7 was followed by a gradual decrease on days 14, 21, and 28, with the phosphate concentration declining to approximately 0.058 mg/L by day 28. The phosphate concentration increased during the first week and reached its peak on day 7, as shown in Table 5. This indicates that phosphate in the copolymer is easily released at the early stage of immersion, likely because it is readily soluble or located near the surface of the material.

After day 7, the measured phosphate concentration decreased. This decline does not necessarily indicate complete depletion of phosphate from the composite, but may reflect depletion of readily diffusible surface-associated phosphate species, combined with dilution effects from periodic medium replacement during sampling. Similar release behavior has been reported for polymer-based slow-release fertilizers, where an initial diffusion-controlled release from surface-accessible regions is followed by a slower release governed by matrix interactions and internal diffusion processes [39].

In contrast to phosphate, nitrogen release followed a slower pattern and reached its maximum on day 14. Nitrogen concentrations on day 1 were relatively low (1.321 and 1.397 mg/L), increased by day 7, and peaked at 3.09 and 3.07 mg/L on day 14, before gradually declining to 2.465 mg/L on day 21 and further by day 28, as shown in Table 6. This gradual release behavior is likely associated with a swelling-controlled, matrix-relaxation process in the copolymer, in which water penetration and network relaxation precede the sustained diffusion of nitrogen-containing species, rather than purely simple diffusion.

When compared, the two release profiles demonstrate that the MCC-g-PMA/PDMU-KP copolymer functions as a controlled nutrient release material. Phosphate is released earlier and more rapidly, whereas nitrogen release is slower and exhibits an initial lag phase, with the maximum occurring during the second week. This behavior is advantageous for slow-release fertilizer applications, as plants generally require phosphate during early growth stages, while nitrogen demand increases during subsequent vegetative growth phases. Moreover, the duplicate measurements for both parameters exhibit low variation, meeting the SNI

precision criterion (relative difference <5%). This confirms that the measurements are stable and not significantly affected by matrix interference from the copolymer.

In cellulose-based and urea–formaldehyde-derived slow-release fertilizer systems under non-sink conditions, nutrient release is governed by coupled diffusion and polymer relaxation processes. During the initial stage, water uptake, polymer swelling, and matrix relaxation dominate mass transport, resulting in a delayed concentration maximum. After this peak, the system approaches a swollen quasi-equilibrium state, where re-equilibration between the aqueous phase and the polymer matrix becomes significant. At this stage, a portion of the released phosphate and ammonium ions may re-adsorb onto polar functional groups (–OH, –COOH, –NH–) or redistribute within the swollen polymer network, leading to a gradual decline in the measured aqueous concentration under static conditions. Such non-monotonic release profiles are characteristic of non-Fickian release behavior in polymer-controlled fertilizer systems and hydrogels when cumulative release is not maintained under sink conditions [39, 40]. This interpretation is presented qualitatively and does not imply kinetic model fitting or quantitative determination of transport exponents, as the release data represent instantaneous concentrations rather than cumulative release.

Overall, the gradual nutrient release over 28 days indicates that the copolymer possesses effective nutrient retention and diffusion control for both elements. The distinct release patterns of phosphate and nitrogen further confirm that ion-matrix interaction mechanisms differ within the polymer system, with nitrogen release being influenced by polymer swelling and matrix relaxation, consistent with non-Fickian release behavior reported in polymer-based slow-release fertilizers [2].

4. Conclusion

This study successfully demonstrated the synthesis of a cellulose-based slow-release fertilizer composite utilizing microcrystalline cellulose extracted from coconut husk waste. Sequential chemical treatments effectively removed lignin and hemicellulose, yielding high-purity microcrystalline cellulose suitable for use as a biopolymer matrix. The incorporation of poly(maleic acid) and polydihydroxymethylurea potassium phosphate (PDMU-KP) using citric acid as an interaction agent resulted in the formation of a stable MCC-g-PMA/PDMU–KP copolymer. Structural and morphological characterizations confirmed the successful formation of the copolymer. FTIR analysis verified the presence of ester, amide, and phosphate functional groups, indicating incorporation of maleate-containing polymer segments and integration of nutrient-bearing components within the MCC matrix, likely involving limited grafting, esterification, and intermolecular interactions. SEM observations revealed a dense, agglomerated composite morphology with a rough, layered surface, in which inorganic phosphate particles were embedded and distributed throughout the polymer matrix. EDX analysis confirmed the presence of carbon, nitrogen, oxygen, phosphorus, and potassium in the analyzed surface region, indicating the coexistence of organic polymer-rich and inorganic nutrient-containing domains within the composite. The EDX result reflects the local surface composition of the selected region and suggests a heterogeneous elemental distribution. XRD results showed a reduction in cellulose crystallinity after copolymerization, consistent with the formation of a polymer composite. Nutrient release studies in aqueous media demonstrated controlled and sustained release behavior over a 28-day period. Phosphate exhibited a relatively faster release, with a maximum concentration during the first week, followed by a gradual decrease, whereas nitrogen release occurred more slowly and reached its maximum concentration in the second week. This differential release behavior reflects distinct interactions between nutrients and the polymer matrix and is advantageous for slow-release fertilizer applications. Overall, the MCC-g-PMA/PDMU–KP copolymer shows strong potential as a cellulose-based slow-release fertilizer system derived from locally available coconut husk waste, with promising implications for improving nutrient use efficiency in agricultural applications.

Acknowledgement

The authors gratefully acknowledge financial support for the research activities from the Faculty of Mathematics and Natural Sciences through Hibah Penelitian PNBP (Skema Pembinaan, 2025), funded by Dana RBA FMIPA (Contract No. 4540/UN30.12/HK/2025). The authors also acknowledge publication funding support from the Program Bantuan Publikasi pada Jurnal Bereputasi Tahun 2025, provided by the Direktorat Jenderal Riset dan Pengembangan, Kementerian Pendidikan Tinggi, Sains dan Teknologi.

References

[1] Sari Edi Cahyaningrum, Retno Ariadi Lusiana, Taufik Abdillah Natsir, Fitriari Izzatunnisa Muhaimin, Andika Pramudya Wardana, Amalia Putri Purnamasari, Misni Bin Misran, Synthesis and characterization of chitosan-modified membrane for urea slow-release fertilizers, *Heliyon*, 10, 15, (2024), https://doi.org/10.1016/j.heliyon.2024.e34981

[2] Priya E., Sudipta Sarkar, Pradip K. Maji, A review on slow-release fertilizer: Nutrient release mechanism and agricultural sustainability, *Journal of Environmental Chemical Engineering*, 12, 4, (2024), 113211 https://doi.org/10.1016/j.jece.2024.113211

[3] Badr-Eddine Channab, Ayoub El Idrissi, Younes Essamlali, Mohamed Zahouily, Nanocellulose: Structure, modification, biodegradation and applications in agriculture as slow/controlled release fertilizer, superabsorbent, and crop protection: A review, *Journal of Environmental Management*, 352, (2024), 119928 https://doi.org/10.1016/j.jenvman.2023.119928

[4] Hongwei Zhang, Hongxu Liang, Libin Xing, Wei Ding, Zengchao Geng, Chenyang Xu, Cellulose-based slow-release nitrogen fertilizers: Synthesis, properties, and effects on pakchoi growth,

International Journal of Biological Macromolecules, 244, (2023), 125413 https://doi.org/10.1016/j.ijbiomac.2023.125413

[5] Mani Prabha, Puneet Tiwari, Pankaj Kumar Yadav, Vandana Singh, Devendra Narayan Tripathi, Tulika Malviya, Biopolymeric starch-based matrix: A sustainable platform for slow release fertilizers, *Carbohydrate Research*, 552, (2025), 109474 https://doi.org/10.1016/j.carres.2025.109474

[6] Vladimir Isakov, Elena Vlasova, Vladislav Forer, Jose Kenny, Sergey Lyulin, Analysis of Slow-Released Fertilisers as a Source of Microplastics, *Land*, 14, 1, (2025), 38 https://doi.org/10.3390/land14010038

[7] V. Chaudhary, Nitin Yeshpal, Bio-Polymer Based Slow Release/Control Release Fertilizer, *Research Journal of Agricultural Sciences*, 14, 5, (2023), 1234-1240

[8] Pavitra Thevi Arnandan, Wan Nor Nadyaini Wan Omar, Zhahidah Husna Hassan, Muhammad Sufri Abd Muhaimin, Danish Akmal Jihat@Ahmad, Makam Mba Michele Raissa, Amnani Shamjuddin, Ken-Lin Chang, Nor Aishah Saidina Amin, Novel sequential ozonolysis-hydrolysis treatments for microcrystalline cellulose synthesis from oil palm empty fruit bunch, *Biomass and Bioenergy*, 199, (2025), 107902 https://doi.org/10.1016/j.biombioe.2025.107902

[9] Junu Poudel, Sagar Bhattarai, Namita Nath, Bhaben Tanti, An exclusive review of microcrystalline cellulose: Structure and applications, and limitations, *Materials Today Communications*, 45, (2025), 112247 https://doi.org/10.1016/j.mtcomm.2025.112247

[10] Feng Zhang, Jun Li, Yuanyuan Chen, Shenglan Zhao, Yaping Zhang, Rongmin Wang, Yufeng He, Pengfei Song, Combination of recycled cellulose with nano-thick flower layered double hydroxides: Biomass water retention slow-release fertilizer for sustainable agriculture, *Colloids and Surfaces A: Physicochemical and Engineering Aspects*, 702, (2024), 135144 https://doi.org/10.1016/j.colsurfa.2024.135144

[11] Syed Baseeruddin Alvi, Anil Jogdand, Aravind Kumar Rengan, Cellulose Nanosystems from Synthesis to Applications, in: A. Barhoum (Ed.) *Handbook of Nanocelluloses: Classification, Properties, Fabrication, and Emerging Applications*, Springer International Publishing, Cham, 2020, https://doi.org/10.1007/978-3-030-62976-2_10-1

[12] Sundus Saeed Qureshi, Sabzoi Nizamuddin, Jia Xu, Tony Vancov, Chengrong Chen, Cellulose nanocrystals from agriculture and forestry biomass: synthesis methods, characterization and industrial applications, *Environmental Science and Pollution Research*, 31, 49, (2024), 58745-58778 https://doi.org/10.1007/s11356-024-35127-3

[13] Rohit Rai, Rahul Ranjan, Sonal Kumari, Nirmal De, Prodyut Dhar, Cellulose-based phosphorylated bamboo with slow urea release and lower carbon footprints improves rainfed rice crop productivity in field trials, *International Journal of Biological Macromolecules*, 306, (2025), 141012 https://doi.org/10.1016/j.ijbiomac.2025.141012

[14] Weishuai Wang, Shiqi Yang, Aiping Zhang, Zhengli Yang, Synthesis of a slow-release fertilizer composite derived from waste straw that improves water retention and agricultural yield, *Science of The Total Environment*, 768, (2021), 144978 https://doi.org/10.1016/j.scitotenv.2021.144978

[15] Khai Chyi Teh, Mei Ling Foo, Chien Wei Ooi, Irene Mei Leng Chew, Sustainable and cost-effective approach for the synthesis of lignin-containing cellulose nanocrystals from oil palm empty fruit bunch, *Chemosphere*, 267, (2021), 129277 https://doi.org/10.1016/j.chemosphere.2020.129277

[16] Sayed Majid Lohmousavi, Hossein Heidari Sharif Abad, Ghorban Noormohammadi, Babak Delkhosh, Synthesis and characterization of a novel controlled release nitrogen-phosphorus fertilizer hybrid nanocomposite based on banana peel cellulose and layered double hydroxides nanosheets, *Arabian Journal of Chemistry*, 13, 9, (2020), 6977-6985 https://doi.org/10.1016/j.arabjc.2020.06.042

[17] P. Manimaran, G. Pitchayya Pillai, V. Vignesh, M. Prithiviraj, Characterization of natural cellulosic fibers from Nendran Banana Peduncle plants, *International Journal of Biological Macromolecules*, 162, (2020), 1807-1815 https://doi.org/10.1016/j.ijbiomac.2020.08.111

[18] Indiralekha Suyambulingam, D. Prince Sahaya Sudherson, Sunesh Narayana Perumal, Subash Narayana Perumal, Comprehensive characterization of microcrystalline cellulose from lemon grass (*Cymbopogan citratus*) oil extraction agro-industrial waste for cementitious composites applications, *International Journal of Biological Macromolecules*, 271, (2024), 132644 https://doi.org/10.1016/j.ijbiomac.2024.132644

[19] Onkar Chand, Lalita Chopra, Nirmala Nithya Raju, Nidhi Asthana, Abdul Malik, Azmat Ali Khan, Extraction of micro fibrous cellulose from coconut husk by using chlorine free process: Potential utilization application as a filter aid, *Journal of Molecular Structure*, 1319, (2025), 139325 https://doi.org/10.1016/j.molstruc.2024.139325

[20] Badan Pusat Statistik Kabupaten Seluma, *Produksi Perkebunan Rakyat Menurut Jenis Tanaman di Kabupaten Seluma Tahun 2024*, Badan Pusat Statistik Kabupaten Seluma, Bengkulu, 2024,

[21] Abdul Rahman Singkam, Fadjri Fil Ahli Hady, Ananda Putri Gita Natasya, Nyimas Ajeng Ayu Meilani, Septia Noparis Fadhila, Anjaly Dewi Puspitasari, Mustika Elmi Dayana, Pemanfaatan Sabut Kelapa Melalui Metode *Slow Sand Filtration* Untuk Memenuhi Kebutuhan Air Bersih di Desa Talang Tinggi Seluma, *Jurnal Penelitian dan PengabdianKepada Masyarakat UNSIQ*, 10, 3, (2023), 220-225 https://doi.org/10.32699/ppkm.v10i3.5258

[22] Adrian Woźniak, Ksawery Kuligowski, Lesław Świerczek, Adam Cenian, Review of Lignocellulosic Biomass Pretreatment Using Physical, Thermal and Chemical Methods for Higher Yields in Bioethanol Production, *Sustainability*, 17, 1, (2025), 287 https://doi.org/10.3390/su17010287

[23] Jun Wu, Xueyu Du, Zhibing Yin, Shuang Xu, Shuying Xu, Yucang Zhang, Preparation and characterization of cellulose nanofibrils from coconut coir fibers and their reinforcements in biodegradable composite films, *Carbohydrate Polymers*, 211, (2019), 49-56 https://doi.org/10.1016/j.carbpol.2019.01.093

[24] Shamala Gowri Krishnan, Fei-ling Pua, Fan Zhang, Oil palm empty fruit bunch derived microcrystalline cellulose supported magnetic acid catalyst for esterification reaction: An optimization study, *Energy Conversion and Management: X*, 13, (2022), 100159 https://doi.org/10.1016/j.ecmx.2021.100159

[25] Chidamparam Poornachandhra, Rajamani M. Jayabalakrishnan, Govindaraj Balasubramanian, Arunachalam Lakshmanan, S. Selvakumar, Muthunalliappan Maheswari, Joseph Ezra John, Coconut husk fiber: A low-cost bioresource for the synthesis of high-value nanocellulose, *Biointerface Research in Applied Chemistry*, 13, 6, (2023), 504 https://doi.org/10.33263/BRIAC136.504

[26] Rasaq S. Abolore, Swarna Jaiswal, Amit K. Jaiswal, Green and sustainable pretreatment methods for cellulose extraction from lignocellulosic biomass and its applications: A review, *Carbohydrate Polymer Technologies and Applications*, 7, (2024), 100396 https://doi.org/10.1016/j.carpta.2023.100396

[27] Yang Xiang, Yaqing Liu, Mingshan Gong, Yingfang Tong, Yuhan Liu, Guizhe Zhao, Jianming Yang, Preparation of Novel Biodegradable Polymer Slow-Release Fertilizers to Improve Nutrient Release Performance and Soil Phosphorus Availability, *Polymers*, 15, 10, (2023), 2242 https://doi.org/10.3390/polym15102242

[28] Isha Dudeja, Ramandeep Kaur Mankoo, Arashdeep Singh, Jaswinder Kaur, Citric acid: An ecofriendly cross-linker for the production of functional biopolymeric materials, *Sustainable Chemistry and Pharmacy*, 36, (2023), 101307 https://doi.org/10.1016/j.scp.2023.101307

[29] Halimatuddahliana Nasution, Hamidah Harahap, Nisaul F. Dalimunthe, M. Hendra S. Ginting, Mariatti Jaafar, Orlando O. H. Tan, Hotmauli K. Aruan, Alief L. Herfananda, Hydrogel and Effects of Crosslinking Agent on Cellulose-Based Hydrogels: A Review, *Gels*, 8, 9, (2022), 568 https://doi.org/10.3390/gels8090568

[30] Yu-Jia Hung, Ming-Yen Chiang, En-Tze Wang, Tzong-Ming Wu, Synthesis, Characterization, and Physical Properties of Maleic Acid-Grafted Poly(butylene adipate-co-terephthalate)/Cellulose Nanocrystal Composites, *Polymers*, 14, 13, (2022), 2742 https://doi.org/10.3390/polym14132742

[31] Eka Marya Mistar, Muhammad Muhammad, Ida Hasmita, Tata Alfatah, Sustainable enhancement of vinyl ester nanobiocomposites reinforced with succinylated coconut fiber and rice husk bionanocarbon, *International Journal of Biological Macromolecules*, 337, (2026), 149364 https://doi.org/10.1016/j.ijbiomac.2025.149364

[32] Randis Randis, Djarot B. Darmadi, Femiana Gapsari, Achmad As'Ad Sonief, Isolation and characterization of microcrystalline cellulose from oil palm fronds biomass using consecutive chemical treatments, *Case Studies in Chemical and Environmental Engineering*, 9, (2024), 100616 https://doi.org/10.1016/j.cscee.2024.100616

[33] M. Lakshmipriya, R. Ezhil Vizhi, D. Rajan Babu, Growth and characterization of maleic acid single crystal, *Optik*, 126, 23, (2015), 4259-4262 https://doi.org/10.1016/j.ijleo.2015.08.126

[34] Costas Tsioptsias, Afroditi Panagiotou, Paraskevi Mitlianga, Thermal Behavior and Infrared Absorbance Bands of Citric Acid, *Applied Sciences*, 14, 18, (2024), 8406 https://doi.org/10.3390/app14188406

[35] Jingying Chen, Jing Wu, Theo Veldhuis, Francesco Picchioni, Patrizio Raffa, Cor E. Koning, Mechanistic Study on Citric Acid–Based Esterification: A Versatile Reaction for Preparation of Hydrophilic Polymers, *ACS Sustainable Chemistry & Engineering*, 13, 1, (2025), 559-570 https://doi.org/10.1021/acssuschemeng.4c07569

[36] Swapan Suman, Shalini Gautam, Pyrolysis of coconut husk biomass: Analysis of its biochar properties, *Energy Sources, Part A: Recovery, Utilization, and Environmental Effects*, 39, 8, (2017), 761-767 https://doi.org/10.1080/15567036.2016.1263252

[37] Navdeep Kaur, Parul Chandel, Antonio J. Capezza, Annu Pandey, Richard T. Olsson, Nibedita Banik, Upcycling coconut husk coir by extraction of cellulose nanofibrils using green citric acid from lemon juice, *RSC Sustainability*, 3, 7, (2025), 2970-2983 https://doi.org/10.1039/D5SU00281H

[38] Sunkara Srinivasa Rao, Ikkurthi Kanaka Durga, Chebrolu Venkata Tulasi-Varma, Dinah Punnoose, Lee Jae Cheol, Hee-Je Kim, The synthesis and characterization of lead sulfide with cube-like structure as a counter electrode in the presence of urea using a hydrothermal method, *New Journal of Chemistry*, 39, 9, (2015), 7379-7388 https://doi.org/10.1039/C5NJ01308A

[39] Babar Azeem, KuZilati KuShaari, Zakaria B. Man, Abdul Basit, Trinh H. Thanh, Review on materials & methods to produce controlled release coated urea fertilizer, *Journal of Controlled Release*, 181, (2014), 11-21 https://doi.org/10.1016/j.jconrel.2014.02.020

[40] Dora Lawrencia, See Kiat Wong, Darren Yi Sern Low, Bey Hing Goh, Joo Kheng Goh, Uracha Rungsardthong Ruktanonchai, Apinan Soottitantawat, Learn Han Lee, Siah Ying Tang, Controlled Release Fertilizers: A Review on Coating Materials and Mechanism of Release, *Plants*, 10, 2, (2021), 238 https://doi.org/10.3390/plants10020238